In situ assembled diffraction grating for biomolecular detection

Chun-Li Chang
School of Electrical and Computer Engineering, Purdue University, West Lafayette, Indiana 47907

Ghanashyam Acharya
Birck Nanotechnology Center, Purdue University, West Lafayette, Indiana 47907

Cagri A. Savran[a)]
School of Mechanical Engineering, Purdue University, West Lafayette, Indiana 47907;
School of Electrical and Computer Engineering, Purdue University, West Lafayette, Indiana 47907;
Weldon School of Biomedical Engineering, Purdue University, West Lafayette, Indiana 47907;
and Birck Nanotechnology Center, Purdue University, West Lafayette, Indiana 47907

(Received 11 April 2007; accepted 11 May 2007; published online 5 June 2007)

The authors report experiments with a diffraction-based biosensor based on self-assembly of target-containing nanobeads that form optical diffraction gratings. They demonstrate that the diffraction signal is a function of the bead size, and that noise is minimized by normalizing the intensities of the diffraction modes. They characterize the dependence of the diffraction signal on equivalent bead size and demonstrate the potential of the scheme in detecting biologically significant molecules. © *2007 American Institute of Physics*. [DOI: 10.1063/1.2746409]

The development of rapid and label-free biosensors for the detection of clinical biomarkers is important for early diagnosis of diseases.[1] A variety of optical biosensors have been developed for biomolecular detection.[2,3] Among them, optical-diffraction-based biosensing has been demonstrated to be a powerful method for detecting biomolecular binding, which depends on changes in effective height or refractive index on periodically patterned gratings.[4–9] A few reports discuss the diffraction signal intensities with respect to the grating height shifts.[10–12] In many studies involving diffraction gratings, additional signal enhancement was necessary. The enhancement was achieved either by microfabricating diffraction gratings with specific heights or by using sequential amplification steps after the capture of target molecules on a solid sensor surface. We herein report a study on self-fabricated diffraction gratings with bioconjugated spheres. Accordingly, binding of target-containing beads to a functionalized area directly forms a diffraction grating and inherently provides an enhanced signal without the use of any enzymes, fluorescent, or radio labels. The method is rapid and inexpensive due to its being devoid of integrated circuit fabrication techniques and sequential amplification steps. In this letter, we characterize the dependence of the signal intensity on the bead size and also demonstrate the system's potential for rapid and label-free detection of clinically important biomolecules.

The detection strategy involves the *in situ* assembly of diffraction gratings and interferometry measurements (Fig. 1). On a gold-coated glass slide (gold chip), periodic patterns of biotin-coupled bovine serum albumin (B-BSA) were microcontact printed using a polydimethylsiloxane (PDMS) stamp. These B-BSA micropatterns act as ligand templates for the streptavidin coupled polystyrene beads (streptavidin-beads) to form *in situ* assembled optical diffraction gratings. The interference of coherent light beams reflecting from the bare gold surface and the top of the beads provides the means for optical signal detection. The beads, because of their larger size compared to the target molecules, significantly and intrinsically enhance the signal intensity without the need for additional amplification.

Interference is an optical phenomenon resulting from the superposition of electromagnetic waves traveling with different path lengths. When an ideal reflective diffraction grating is illuminated by a coherent monochromatic light, i.e., laser, the reflected beam from ridges and lands possess different phases and thus diffraction patterns composed of bright and dark modes are produced (Fig. 2). The incident beam on the grating surface has to cover at least four pairs of stripes in order to produce well-separated diffraction modes so that the intensity of each mode could be individually measured.[13] For an ideal diffraction grating shown in Fig. 2, the intensity of zeroth and first order diffraction modes can be represented by Eqs. (1) and (2), respectively.

$$I_0 \propto \cos^2(2\pi\delta/\lambda), \tag{1}$$

$$I_1 \propto \sin^2(2\pi\delta/\lambda). \tag{2}$$

Here, δ represents the height of the grating and λ the wavelength of the laser beam (632.8 nm). Equations (1) and (2) suggest that the intensity of each mode is a periodic function of grating height δ. Therefore, for each grating height (δ) there exists an *equivalent height* (δ') between 0 and $\lambda/4$ that gives the same diffraction signal intensities.

In order to validate the detection strategy, we chose the well-established biotin-streptavidin pair as a model system. The tetrameric protein streptavidin binds to its complementary ligand biotin, in a 1:4 ratio with a high binding affinity ($K_a = 10^{15} M^{-1}$). Micropatterns of biotin ligands on a gold chip were prepared using a PDMS stamp bearing 15 μm wide alternating linear patterns. An ultrasonically cleaned stamp was inked with a solution of B-BSA [Pierce, 1 mg/ml of phosphate buffered saline (PBS, GIBCO)] and left to stand for 5 min. After removing the excess solution on the stamp with a gentle stream of nitrogen gas, the stamp was brought into contact with a precleaned gold chip. A very small amount of force was applied on the stamp to make a

[a)]Electronic mail: savran@purdue.edu

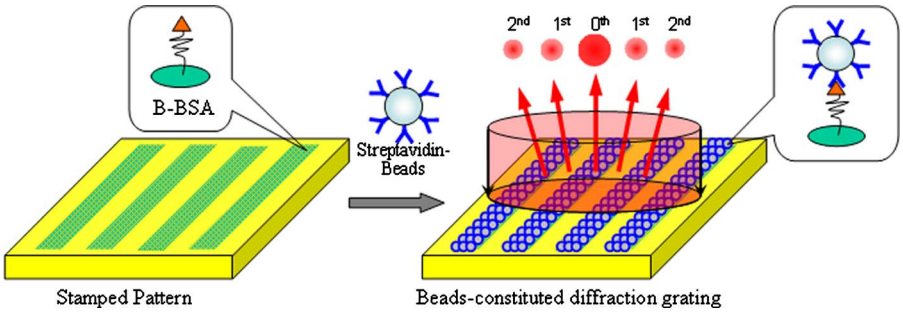

FIG. 1. (Color online) Schematic of the *in situ* assembled diffraction grating as a biosensor.

contact between both surfaces. The stamp was removed after 2 min and the stamped gold surface was rinsed gently with PBS to remove the unbound B-BSA. The B-BSA was deposited only in the direct contact areas on the gold surface. Due to the strong binding of BSA to gold surface, the stamping provided robust micropatterns with a high density of biotin. The gold chip containing B-BSA patterns was incubated with a suspension of streptavidin-coupled polystyrene beads (Bangs, 30 μl, 1.5×10^{12} beads/ml) for 5 min followed by rinsing with PBS and nanopure water to remove unbound streptavidin beads, and dried under a gentle stream of nitrogen gas. This step yielded well defined micropatterns of beads that functioned as diffraction gratings (Fig. 3). Note that the streptavidin on the beads served as model "targets" in this study. The method is otherwise generic: any target molecule can be captured using beads functionalized with appropriate receptors.

To examine the effect of grating height on the signal intensity, we used polystyrene streptavidin beads with various mean diameters: 120, 310, 350, 390, and 490 nm (350 nm beads were magnetic polystyrene). The equivalent bead size, i.e., the ideal diffraction grating height between 0 and $\lambda/4$ that would produce the same diffraction intensities are 120, 6, 34, 74, and 143 nm, respectively. The gratings formed by beads with different diameters were examined by atomic force microscopy to be correspondent with the nominal mean bead sizes.

The interferometry setup comprised of a helium-neon laser beam (Newport R-30991, 632.8 nm, 5 mW) focused onto the sample surface by a convex lens (focal length: 60 mm) to a beam diameter of approximately 150 μm. The reflected laser beam was guided onto a silicon photodiode by a beam splitter (Thorlabs BS016). A pair of convex lenses (focal lengths: 30 and 70 mm) fixed between the beam splitter and photodiode further separated the diffraction modes. A silicon photodiode (12 V reverse bias, Thorlabs DET110) in conjunction with an adjustable aperture (Thorlabs SM1D12) and a bandpass filter (Thorlabs FL632.8-10) was affixed on a translation stage (Thorlabs MT3) for measuring the signal intensities. The photodiode was connected to a 10 kΩ resistor to convert the output current into voltage. The resulting signal was connected to a low-pass filter/amplifier (Stanford Research SR640) and recorded by a computer with a National Instruments LABVIEW interface.

Neat B-BSA patterns did not produce a measurable diffraction pattern upon irradiation with the laser beam. However, the reflected beam from the bead-constituted diffraction gratings formed distinct and measurable diffraction patterns composed of several order modes. The intensities of the zeroth and first modes (I_0 and I_1) were measured with 10 and 30 dB gains, respectively, and were plotted against the equivalent bead sizes (Fig. 4). According to Eqs. (1) and (2) I_0 decreases and I_1 increases with increasing equivalent bead size. Figure 4(a) shows that individual variations of I_0 and I_1 with equivalent bead size are inconsistent with the theoretical expectation. We attribute this to sample-to-sample variations, small drifts in incident laser intensity, and a few important differences between the current system and an ideal diffraction grating (which we describe next). However, the normalized modal intensities (I_1/I_0) and the associated curve fit shown in Fig. 4(b) agree with the expected trend that I_1 increases with respect to I_0 with increasing equivalent bead size.

Our diffraction gratings are composed of randomly distributed spherical beads and not solid ridges with rectangular cross sections. The effective roughness of the bead patterns is much higher in comparison and thus degrades the diffraction intensity due to scattering. Further, the imperfect occupation ratio of beads also affects the diffraction intensity. In our experiments, we obtained an average of 63% occupation ratio for each sample with only minor variation. Moreover, the polydispersity of the bead diameters and nonspecific binding of beads to some extent in the interpattern regions may also affect the diffraction mode intensities. Also, small variations between samples and drifts in laser intensity make it difficult to rely on absolute measurements of the diffraction modes. Because of these deviations from ideal conditions, it is not possible to have a perfect agreement with

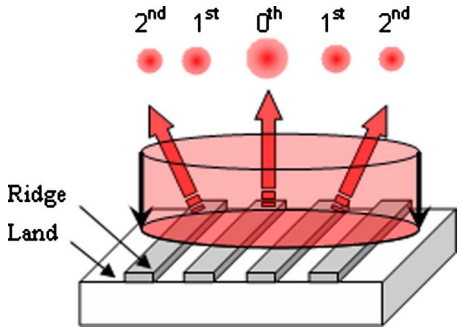

FIG. 2. (Color online) Operation basics of an ideal diffraction grating.

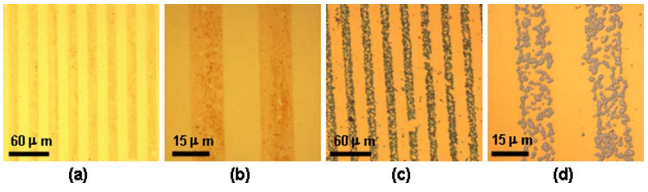

FIG. 3. (Color online) Optical micrograph of [(a) and (b)] neat B-BSA stamped patterns and [(c) and (d)] the gratings obtained from the self-assembly of streptavidin-coated beads with 490 nm diameter on B-BSA micropatterns printed on a gold chip.

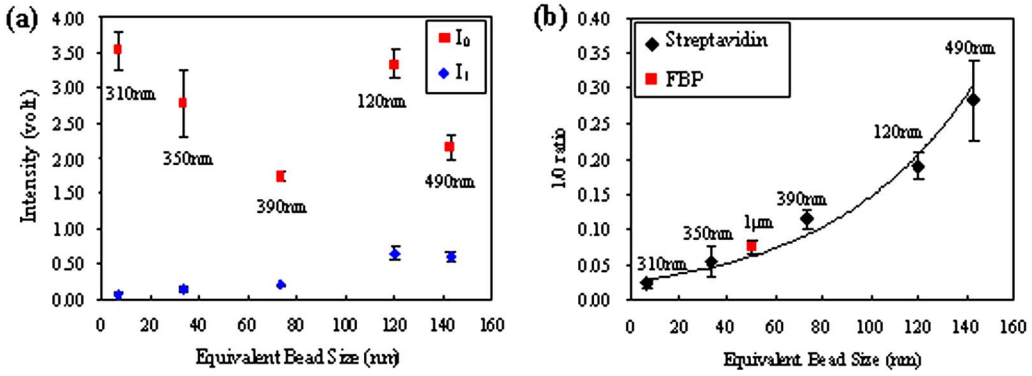

FIG. 4. (Color online) Experimental results. (a) Variation of the intensities of the zeroth and first modes (I_0 and I_1) with equivalent bead size. (b) Dependence of I_1/I_0 ratio on equivalent bead size and the signal resulting from cancer marker (FBP) detection.

theoretical expectations. However, normalizing the intensities (I_1/I_0) significantly reduces disturbances sustained by absolute measurements and confirms the expected increase of I_1 with respect to I_0 with increasing equivalent bead size. Moreover, the plot shown in Fig. 4(b) serves as a characteristic curve to predict a signal for a specific equivalent bead size (and vice versa).

In order to verify the obtained characteristic curve, we prepared a diffraction grating using streptavidin-coated magnetic beads with a diameter (860 nm) different from the ones used before. A bead with an actual diameter of 860 nm (equivalent diameter=124 nm) should result in a I_1/I_0 ratio similar to that of the 120 nm bead grating. This indeed was the case: the experimentally measured I_1/I_0 ratio was 0.181, while that for 120 nm bead grating was 0.190. The slightly lower signal value of 860 nm bead grating could be attributed to the higher surface roughness of the bead patterns due to the larger bead size leading to increased scattering. These results suggest that the intensity of each mode depends on the grating height and verify the characteristic curve in Fig. 4(b).

To demonstrate the potential of this strategy in clinical diagnostics, we chose folate binding protein (FBP) (Scripps Research Institute), a cancer biomarker circulating in blood,[14] as a model system. It is known that FBP specifically binds to folic acid with strong affinity.[14] We microcontact printed patterns of folate coupled bovine serum albumin (F-BSA) on a gold chip as molecular-recognition elements that binds specifically to FBP. Meanwhile, the FBP present in a PBS solution was captured by FBP-antibody-coupled polystyrene microbeads (1 μm mean diameter). The FBP-bound bead suspension (1.5×10^{12} beads/ml) was introduced to the F-BSA stamped gold chip and was incubated for 10 min followed by rinsing with PBS and nanopure water and drying under a gentle stream of nitrogen gas. Upon illuminating the sample surface, a clear diffraction pattern was observed confirming the presence of the target molecules on the beads. The I_1/I_0 ratio was measured to be 0.076 and plotted against the equivalent bead size (51 nm) [Fig. 4(b)]. The I_1/I_0 ratio of FBP experiment is in good agreement with the characteristic curve we obtained earlier.

In conclusion, we have studied a rapid, label-free, and inexpensive diffraction biosensor based on *in situ* assembled diffraction gratings. The optical processing and data analysis were straightforward and fluorescence or radio label-free. Under similar bead packing densities, we characterized the dependence of modal ratios upon an *equivalent bead size*. This characteristic dependence enabled us to choose beads with proper sizes for stronger signals and also allowed verification of bead sizes. We also demonstrated the potential of the system as a diagnostic tool by detecting FBP, a cancer biomarker. The system is generic and can be used to detect numerous biomarkers by functionalizing beads and the solid surface with appropriate receptors. The system can also be readily combined with bead-based separation techniques (e.g., immunomagnetic separation) to capture molecules from complicated mixtures. We anticipate that this biosensor, because of its simplicity and potential to miniaturization, can facilitate the development of an inexpensive and portable device.

[1]M. Ferrari, Nat. Rev. Cancer **5**, 161 (2005).
[2]F. S. Ligler and C. A. R. Taitt, *Optical Biosensors: Present and Future*, 1st ed. (Elsevier Science, Amsterdam, Netherlands, 2002).
[3]J. Gooding, Anal. Chim. Acta **559**, 137 (2006).
[4]R. Jenison, S. Yang, A. Haeberli, and B. Polisky, Nat. Biotechnol. **19**, 62 (2001).
[5]J. B. Goh, R. W. Loo, R. A. Mcaloney, and M. C. Goh, Anal. Bioanal. Chem. **374**, 54 (2002).
[6]J. B. Goh, P. L. Tam, R. W. Loo, and M. C. Goh, Anal. Biochem. **313**, 262 (2003).
[7]J. B. Goh, R. W. Loo, and M. C. Goh, Sens. Actuators B **106**, 243 (2005).
[8]R. W. Loo, P. L. Tam, J. B. Goh, and M. C. Goh, Anal. Biochem. **337**, 338 (2005).
[9]P. T. Fiori and M. F. Paige, Anal. Bioanal. Chem. **380**, 339 (2004).
[10]M. M. Varma, H. D. Inerowicz, F. E. Regnier, and D. D. Nolte, Biosens. Bioelectron. **19**, 1371 (2004).
[11]M. M. Varma, D. D. Nolte, H. D. Inerowicz, and F. E. Regnier, Opt. Lett. **29**, 950 (2004).
[12]L. Peng, M. M. Varma, F. E. Regnier, and D. D. Nolte, Appl. Phys. Lett. **86**, 183902 (2005).
[13]G. G. Yaralioglu, A. Atalar, S. R. Manalis, and C. F. Quate, J. Appl. Phys. **83**, 7405 (1998).
[14]W. A. Henne, D. D. Doorneweerd, J. Lee, P. S. Low, and C. Savran, Anal. Chem. **78**, 4880 (2006).